Mechanisms of Organocatalytic Amidation and Trans-Esterification of Aromatic Esters As a Model for the Depolymerization of Poly(ethylene) Terephthalate

ARTICLE *in* THE JOURNAL OF PHYSICAL CHEMISTRY A · DECEMBER 2012

Impact Factor: 2.69 · DOI: 10.1021/jp304212y · Source: PubMed

THE JOURNAL OF PHYSICAL CHEMISTRY A

Article

pubs.acs.org/JPCA

Mechanisms of Organocatalytic Amidation and Trans-Esterification of Aromatic Esters As a Model for the Depolymerization of Poly(ethylene) Terephthalate

Hans W. Horn,*[,†] Gavin O. Jones,[†] DiDi S. Wei,[†,‡] Kazuki Fukushima,[†,§] Julien M. Lecuyer,[†,∥] Daniel J. Coady,[†] James L. Hedrick,[†] and Julia E. Rice[†]

[†]IBM Almaden Research Center, 650 Harry Road, San Jose, California 95120, United States

[‡]Physics and Astronomy Department, University of Denver, Denver, Colorado 80208, United States

[§]Department of Polymer Science and Engineering, Yamagata University, 3-4-16 Jonan, Yonezawa, Yamagata 992-8510, Japan

[∥]Chemical and Materials Engineering Department, San Jose State University, San Jose, California 95192, United States

Supporting Information

ABSTRACT: We describe investigations with B3LYP density functional theory to probe mechanisms for the organocatalyzed depolymerization of poly(ethylene) terephthalate (PET) into ester and amide products. These investigations utilize model systems involving the trans-esterification and amidation of methylbenzoate (MB) with ethylene glycol (EG), ethylenediamine (EDA), and ethanolamine (EA) organocatalyzed by 1,5,7-triazabicyclododecene (TBD) and 1,8-diazabicyclo[5.4.0]undec-7-ene (DBU). Mechanisms for reactions in which TBD acts as the lone catalyst have been compared with pathways in which TBD and DBU catalyze these processes with an additional molecule of the amine or alcohol acting as a cocatalyst. Calculations suggest that the combination of an organocatalyst with a molecule of an alcohol or amine cocatalyst is slightly more activating than a lone catalyst. Our results predict that nucleophilic attack is the rate-determining step in reactions involving EDA and EG and that TBD is a better catalyst than DBU in the amidation of MB with EDA; in addition, both organocatalysts activate alcohols more than amines during nucleophilic attack. Amidation and trans-esterification possess similar barriers for reactions involving EA; but the amide, which is the thermodynamic product, is preferentially formed instead of the ester.

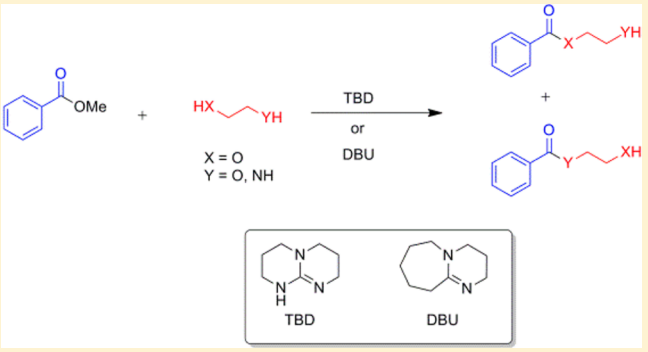

INTRODUCTION

According to recent estimates, the amount of plastic waste generated in the US constitutes 12% of the municipal solid waste (MSW) sent to landfills, a percentage only smaller than the amount generated by paper, food scraps, and yard trimmings.[1] Poly(ethylene) terephthalate (PET) (Scheme 1a), a thermoplastic that is widely used in packaging products, constitutes a large fraction of the total plastic refuse generated as MSW and the amount of waste PET generated per year is likely to increase.[2] The recycling of petroleum-based plastics such as PET has attracted enormous attention, yet only 28% of PET products are recycled, usually by mechanical or, less commonly, chemical processes.[3−8] Mechanical recycling of PET leads to products with inferior material properties and is, therefore, less appealing than chemical recycling.[2,9−13]

Chemical recycling involves depolymerization of the plastic into its constituent monomers followed by purification and subsequent repolymerization to yield high-quality plastics.[7,8] Depolymerization of PET has traditionally been accomplished by the use of metal-based catalysts.[9−15] The use of organocatalysts in the chemical processing of PET offers a diversity of mechanistic pathways that can provide new opportunities for selective depolymerization and polymerization processes, advantages not afforded by transition metal catalysis.[16−18] In addition, purification of the monomers formed from organocatalysis is less expensive than purification of monomers made by organometallic catalysis.

Scheme 1

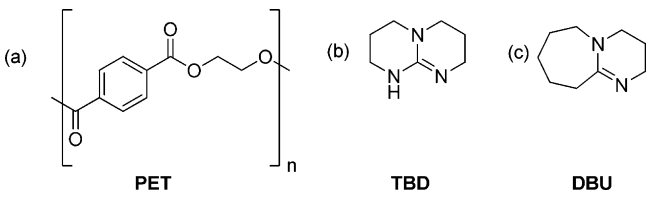

Received: May 1, 2012
Revised: November 27, 2012
Published: November 28, 2012

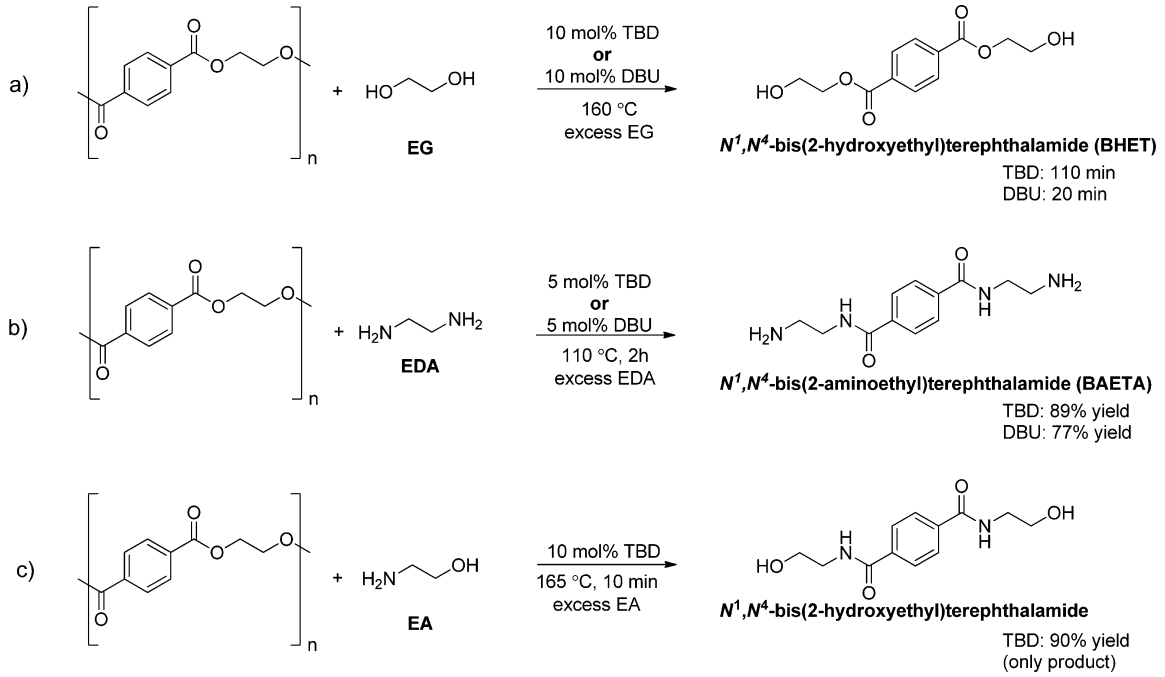

Figure 1. TBD- and DBU-catalyzed trans-esterification and amidation reactions of PET with (a) ethylene glycol (EG), (b) ethylene diamine (EDA), and (c) ethanolamine (EA).[25].

In recent reports, our lab demonstrated that the guanidine and amidine bases, 1,5,7-triazabicyclododecene (TBD) and 1,8-diazabicyclo[5.4.0]undec-7-ene (DBU) (Scheme 1b,c), catalyze the ring-opening polymerization (ROP) of lactides and other cyclic esters.[19−24] Inspired by these results, we more recently demonstrated that TBD catalyzes the depolymerization of PET by processing with ethylene glycol (EG) to form the monomeric diester N^1,N^4-bis(2-hydroxyethyl)terephthalester (BHET) as the major product (Figure 1a).[25] Apart from the obvious environmental benefits, the depolymerization of PET may also potentially lead to the formation of monomers or oligomers with useful properties. For example, we have depolymerized PET with amines such as ethylenediamine (EDA) to form the analogous diamide N^1,N^4-bis(2-aminoethyl)terephthalamide (BAETA) (Figure 1b).[26] Such diamides are useful as monomers for highly thermostable polymers utilized as hardeners or modifiers for epoxy resins.[27,28]

We have performed laboratory experiments to compare the reactivities of TBD and DBU in reactions of EG and EDA with PET.[25,29] Reactivities were evaluated as the time observed for reaction completion (i.e., when PET flakes disappear) or on the yields of product formed in a set duration of reaction (See Supporting Information for details). The glycolysis of PET at 160 °C is complete after 20 min in the presence of DBU but is only complete after 110 min in the presence of TBD.[29] These results signify that DBU catalyzes the glycolysis of PET at a faster rate than TBD. In contrast, the TBD-catalyzed amidation of PET by EDA appears to be more efficient than that catalyzed by DBU. The yields of the diamide product formed in reactions catalyzed by TBD and DBU are 89% and 77%, respectively (Figure 1b).[25]

We have also experimentally investigated the TBD-catalyzed depolymerization of PET with ethanolamine (EA) to gain some insights into the relative reactivities of the alcohols and amines in these reactions. Interestingly, only the diamide is formed in this reaction and not the diester (Figure 1c), signifying that the rate of amidation is faster than the rate of trans-esterification or that trans-esterification is reversible and the diamide is the thermodynamic product formed in the reaction.

We previously employed theoretical investigations to determine why TBD is so efficient at catalyzing the ROP of L-lactide[24,30] and depolymerizing PET with EG.[25] We found that the preferred mechanisms in both ROP and depolymerization relied on the bifunctional nature of TBD involving the formation of hydrogen-bonding interactions between the reactants and key hydrogen-bond donor and acceptor sites on the organocatalyst that facilitate nucleophilic attack and ester formation. Such dual activation processes have also been proposed for systems involving the combination of a thiourea/amine base in which the thiourea hydrogen-bonds to the ester, while the amine base activates the nucleophile for attack on the ester.[31] These results are in agreement with studies carried out by other groups on similar reactions.[32−34]

Herein, we report studies that extend our previous theoretical studies on mechanisms involving the TBD-catalyzed depolymerization of PET with EG for which we have considered alternative mechanisms. We have also investigated a number of mechanisms for the depolymerization of PET with EDA and EA. Finally, we make comparisons between reactions catalyzed by TBD with those catalyzed by DBU.

COMPUTATIONAL METHODOLOGY

All reactions were performed with GAMESS-US[35,36] using B3LYP density functional theory.[37−40] Geometry optimizations were performed with the 6-31+G(d) basis set[41−43] followed by single-point energy calculations with the aug-cc-pVTZ basis set.[44,45] This was done in accordance with calculations performed on selected species with the VTZP+ basis set[46] to validate the 6-31+G(d) basis set (see Supporting Information for details). These results suggested that the 6-31+G(d) basis set is sufficient for geometry optimizations, but a larger basis set

dx.doi.org/10.1021/jp304212y | J. Phys. Chem. A 2012, 116, 12389−12398

is required for more accurate energy calculations. While many conformations of intermediates and transition states were investigated, only mechanisms and structures corresponding to the lowest energy pathways are discussed herein.

A continuum dielectric with the IEF-cPCM method[47,48] was utilized to represent reaction conditions. Only the electrostatic term was included. All geometry optimizations were performed with the PCM solvent model. PCM parameters (solvent radius and dielectric) for some of the reactants/solvents in question under the experimental conditions do not exist. We used the radius of a similarly sized known solvent to determine the solvent radii.[49] In so doing, we discovered a correlation between the size of common solvent molecules and their PCM solvent radii (as implemented in GAMESS/US). We estimated the PCM solvent radii for the solvents in question using this correlation. Estimated PCM radii are shown in Table 1 along with the dielectric, ε, for which we used equations of state to extrapolate $\varepsilon(1/T)$ to the temperature under which the reactions are conducted experimentally.[50]

Table 1. Estimated PCM Radii and Dielectric Constants at Reaction Temperatures for Ethylene Glycol, Ethanolamine, and Ethylenediamine

solvent	PCM radius [Å]	dielectric ε (@ T [°C])[a,b]
ethylene glycol	2.35	19.1 (@ 185)
ethanolamine	2.35	13.0 (@ 170)
ethylenediamine	2.40	8.90 (@ 115)

[a]Experimental temperatures, ref 25. [b]Dielectric constants at experimental temperatures were determined by the equation of state, $\varepsilon(T) = a + bT + cT^2$.[50]

Reported free energies are in kcal/mol. Only vibrational free energy corrections to the electronic energy at the experimental temperatures were used in accordance with recommendations for molecules optimized in implicit solvent.[51] Intrinsic reaction coordinate (IRC) calculations were performed to verify that transition states are connected to the minima that lie on the potential energy surfaces for the reactions; the results of these calculations are shown in the Supporting Information. In addition, normal modes of all structures were examined to verify that ground states possess no imaginary frequencies and that transition structures possess one imaginary frequency corresponding to bond formation or bond breaking. Values of the imaginary frequencies found for each transition structure and relevant bond-breaking/bond-forming distances are contained in the Supporting Information that accompanies this article.

To make this computational study more tractable, we chose the simplest arylester, methylbenzoate (MB), as a model for PET and investigated reactions of MB with EDA, EG, and EA (Scheme 2).[52] To elucidate the origins of the differing reactivities of TBD and DBU, we have compared mechanisms involving both catalysts. Like our previous study on the glycolysis of PET,[25] we have performed investigations on mechanisms in which TBD acts as a lone catalyst in these reactions. We also speculated that the amine and alcohol reagents may play an additional role in catalysis since they are required in large excess in these reactions. This could be especially pertinent for reactions involving the DBU catalyst since, unlike TBD, it is not bifunctional and lacks a proton donor site that can be used to activate both the ester and the amine or alcohol reagent. Consequently, calculations were performed on systems in which an additional molecule of the amine or alcohol acts as a cocatalyst that stabilizes key intermediates and transition states in concert with the TBD or DBU catalyst.

RESULTS AND DISCUSSION

Overview of Reaction Profiles for Amidation and Trans-Esterification of MB. If the type of catalyst or the identity of the alcohol or amine reagent is disregarded, it is apparent that the mechanisms for trans-esterification and amidation possess very similar reaction profiles. For the purpose of summarizing the salient features of these mechanisms, we show an idealized representation of the key stationary points for amidation or trans-esterification in Figure 2 for which we have dispensed with the identity of the amine or alcohol reagent, type of catalyst, and associated energies. Note

Scheme 2

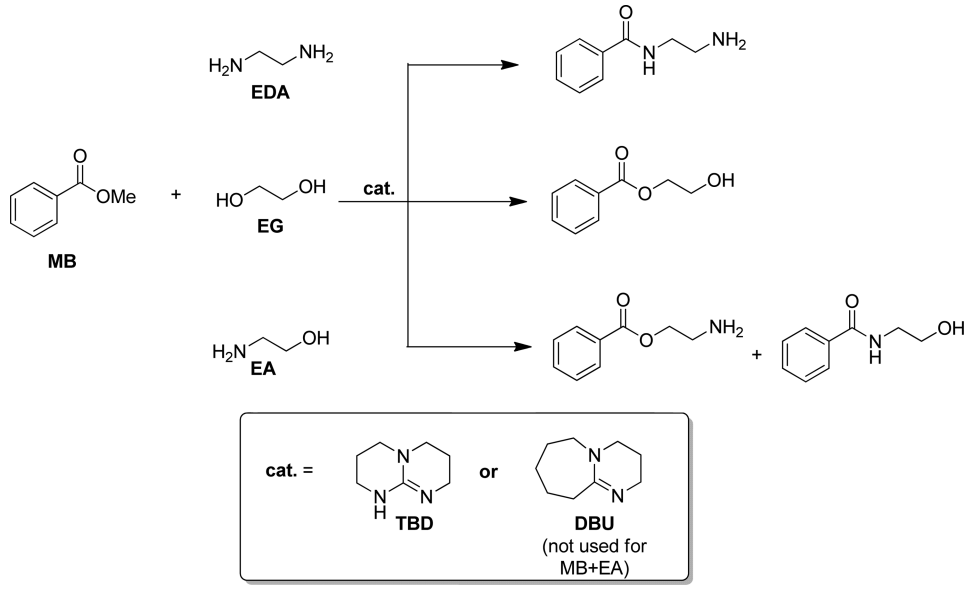

dx.doi.org/10.1021/jp304212y | J. Phys. Chem. A 2012, 116, 12389−12398

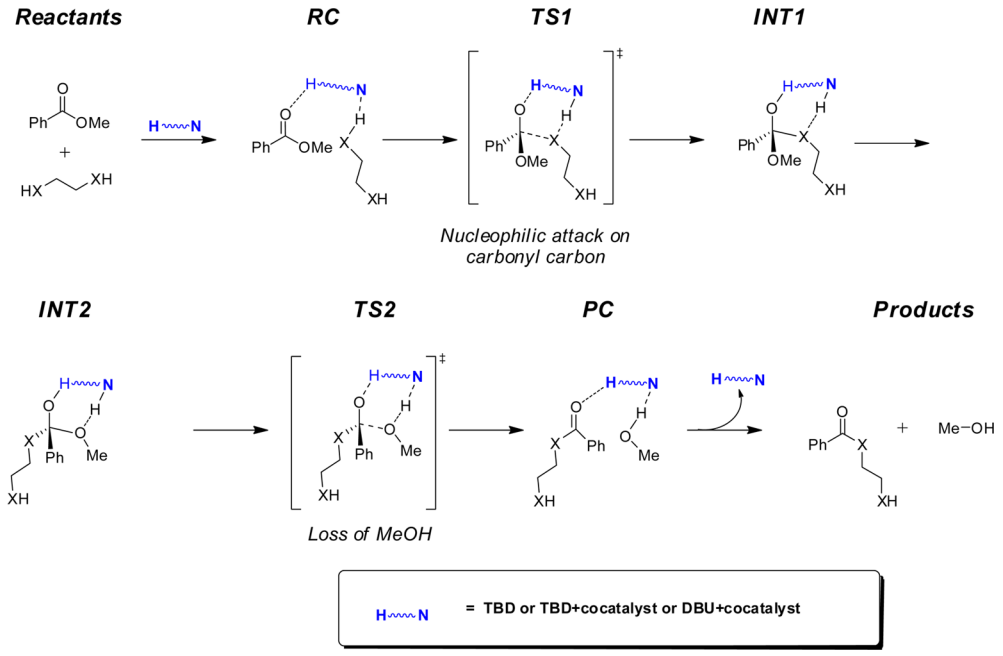

Figure 2. Idealized mechanism for organocatalyzed trans-esterification and amidation of MB.

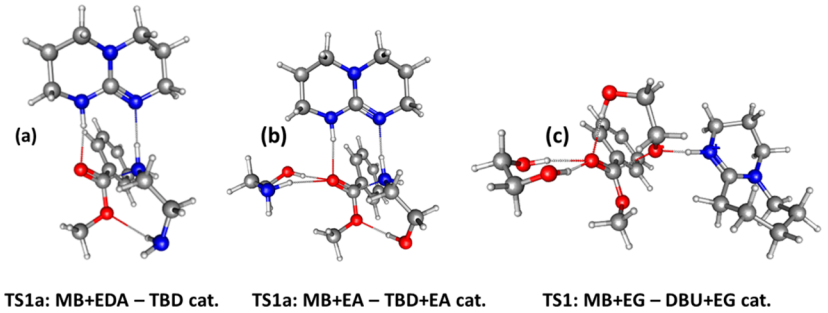

Figure 3. Transition state geometries for the nucleophilic attack of (a) EDA on MB catalyzed by TBD, (b) EA on MB catalyzed by TBD (amidation pathway), and (c) EG on MB catalyzed by DBU.

that the drawings in Figure 2 are idealized structures and that the actual arrangement of organocatalysts and cocatalysts around the reactants vary to some degree. This is illustrated by Figure 3, which shows that the positions of the organocatalysts and cocatalyst are different in computed transition structures for the initial nucleophilic attack of EDA on MB catalyzed by TBD, EA on MB catalyzed by TBD + EA cocatalyst (amidation pathway), and EG on MB catalyzed by DBU + EG cocatalyst, respectively.

The initial step in these mechanisms involves the formation of reactant complexes (RC) in which the organocatalyst (and cocatalyst, as the case may be), the amine or alcohol reagent, and the ester are bound to each other by weak intermolecular interactions such as hydrogen-bonding and dispersion forces. The catalysts in these complexes hold reactants poised for nucleophilic attack in TS1 in which the amine or alcohol reagent is being deprotonated by an organocatalyst, while the carbonyl oxygen is hydrogen-bonded to the same organocatalyst or to a cocatalyst. INT1, which is formed from TS1, is a tetrahedral intermediate in which the oxygen atom that formerly belonged to the carbonyl group of the ester and the N or O atom previously belonging to the amine or alcohol reagent are hydrogen-bonded to the catalyst or to a cocatalyst. Note that nucleophilic attack in reactions involving amidation by EDA and EA occurs in two distinct stages, which we have abridged to TS1 and INT1 in Figure 2 for brevity. Initial C−N bond formation occurs in TS1a, leading to INT1a. The N−H group in INT1a is then deprotonated in TS1b forming INT1b.

INT1 reorganizes to form INT2 in which the catalyst becomes hydrogen-bonded to the oxygen belonging to the leaving methoxy group. TS2 involves the transfer of a proton from the catalyst to the leaving methanol molecule, concomitant with breaking the ester C−O bond as well as the hydrogen-bond to the carbonyl oxygen present in the ester or amide product. This leads to the formation of the product complex, PC, in which the organocatalyst is bound to methanol and the ester or amide product. The organocatalyst reenters the catalytic cycle after release of the methanol byproduct and the ester or amide.

The catalytic activity and chemoselectivity observed in these reactions is largely dependent on the H-donor strength of the amine and alcohol reagents as well as the ability of the catalysts to activate them for nucleophilic attack. Specifically, the presence of the basic catalyst in these reactions can modulate the reactivities of the amine or alcohol reagents so that alcohols become more reactive than amines even though the reverse is true when no organocatalyst is present. These considerations become significant when rationalizing the reactivity trends of

dx.doi.org/10.1021/jp304212y | J. Phys. Chem. A 2012, 116, 12389−12398

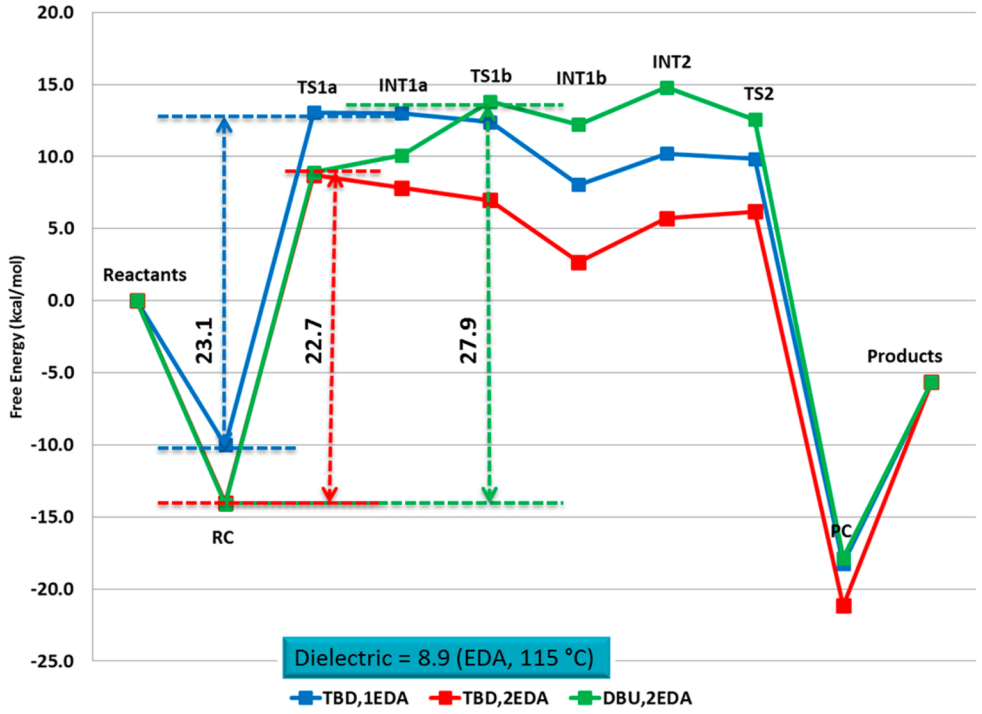

Figure 4. Reaction profiles for the amidation of MB with EDA catalyzed by TBD, TBD + EDA, and DBU + EDA.

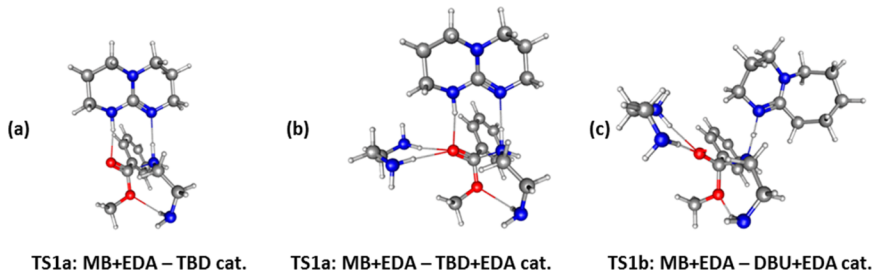

Figure 5. Transition structures for nucleophilic attack of EDA on MB catalyzed by (a) TBD, (b) the TBD + EDA cocatalyst, and (c) the DBU + EDA cocatalyst.

paramount interest to this study. Alcohols are expected to be more easily deprotonated than amines and trans-esterification is expected to be more favorable than amidation if nucleophilic attack is rate-determining.

B3LYP predicts that the product complexes are the global energy minima on the free energy surface but that the reactant complexes formed by the combination of organocatalyst + amine/alcohol reagent and MB are the lowest energy structures prior to formation of the product complex; consequently, all reported barriers are with respect to the reactant complexes. The introduction of a cocatalyst typically lowers the energies of the intermediates and transition states for the majority of these reactions. The transition states for nucleophilic attack (TS1 or TS1a) are rate-determining in nearly all cases with the exception of the TBD-catalyzed esterification reaction of MB with ethanolamine; transition states for ester formation (TS2) are rate-determining in these cases. In addition, for the amidation of EDA by the catalyst combination of DBU + EDA, TS1b involving proton transfer from the N−H group of EDA to DBU is rate-determining.

Amidation of MB with EDA. Three reaction profiles for the amidation of MB by EDA are shown in Figure 4. These involve amidation (1) catalyzed by TBD, (2) catalyzed by the combination of TBD + EDA, and (3) catalyzed by DBU + EDA. The reaction of EDA with MB is exergonic by ∼5 kcal/mol with reference to the reactants, suggesting that there is an appreciable driving force for the formation of the amide product. Reactant complexes formed by the complexation of EDA with the organocatalyst and MB or MB + EDA are stabilized by 10 to 14 kcal/mol with respect to the reactants. Nucleophilic attack during initial amidation involves two stages initiated by attack of the amine reagent on the carbonyl carbon of the ester group in TS1a followed by transfer of the proton attached to the amine reagent to TBD in TS1b. The rate-determining step is TS1a in mechanisms involving catalysis by TBD or by TBD + EDA. In contrast, the rate-determining step in the reaction catalyzed by DBU + EDA is TS1b, presumably due to the fact that DBU is less basic than TBD.

The reaction involving the TBD + EDA catalyst combination leads to the most favorable reaction with a barrier of 22.7 kcal/mol. When TBD acts as the lone catalyst, the barrier increases slightly to 23.1 kcal/mol. In contrast, the reaction involving the DBU + EDA catalyst combination has a barrier of 27.9 kcal/mol. The fact that reactions involving TBD possess lower barriers than that involving DBU is in agreement with the experimental observation that TBD is a more active catalyst

dx.doi.org/10.1021/jp304212y | J. Phys. Chem. A 2012, 116, 12389−12398

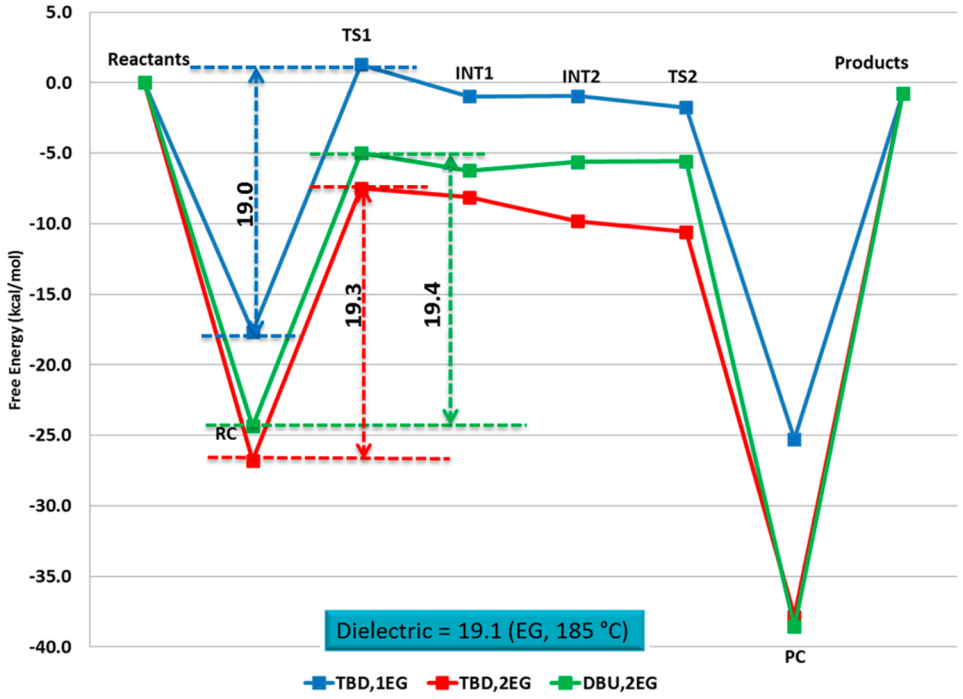

Figure 6. Reaction profiles for the trans-esterification of MB with EG catalyzed by TBD, TBD + EG, and DBU + EG.

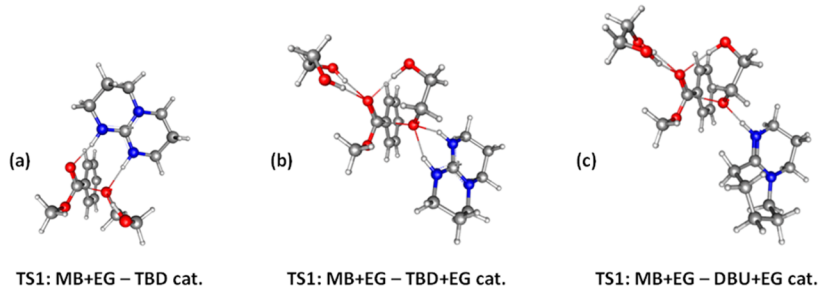

Figure 7. Transition structures for the nucleophilic attack of EG on MB catalyzed by (a) TBD, (b) the TBD + EG cocatalyst, and (c) the DBU + EG cocatalyst.

than DBU in the depolymerization of PET with EDA (Figure 1b).

The fact that reactions involving TBD and TBD + EDA are more kinetically favorable than that involving DBU + EDA is best rationalized by examination of geometric features in the key transition structures for nucleophilic attack of EDA on the ester (Figure 5). TBD is oriented so that it hydrogen-bonds to the carbonyl oxygen of the ester and also with the amine reagent in both transition structures. This orientation is preserved when EDA participates as the cocatalyst by forming bidentate hydrogen-bonds with the carbonyl oxygen. These interactions provide additional stabilization of the negative charges that develop at the carbonyl oxygen atoms in the transition states of the reactions. Since DBU cannot provide this bifunctional interaction, this additional stabilization is absent in the transition state involving DBU.

Interestingly, the presence of the additional EDA molecule only lowers the barrier by 0.4 kcal/mol when the transition structure involving TBD is compared with that involving TBD + EDA. It appears that, while the transition structure is stabilized by the addition of a cocatalyst, the reactant complex is stabilized to almost the same extent.

Trans-Esterification of MB with EG. The reaction profiles for the trans-esterification of MB with EG are shown in Figure 6. The mechanism involving TBD as the lone catalyst has been compared with mechanisms involving a molecule of EG acting as a cocatalyst in combination with TBD and DBU. The glycolysis of MB is almost energy neutral, suggesting that driving forces such as the high reaction temperature and the large excess of ethylene glycol used in the laboratory experiments facilitates reaction completion.

Steps involving nucleophilic attack of EG on MB, TS1, are rate-determining in mechanisms involving TBD as the lone catalyst, or involving the TBD + EG or DBU + EG cocatalyst systems. The barriers of these processes are all predicted to be approximately 19 kcal/mol, suggesting that the rates of all of these reactions are only slightly affected by the nature of the catalyst.

Close examination of the geometries of the rate determining transition states involving nucleophilic attack (Figure 7) reveals significant differences in the orientations and hydrogen-bonding interactions involving the ester, the attacking diol, and the catalysts. As the lone catalyst, TBD deprotonates the attacking hydroxyl group while forming a hydrogen-bond with the carbonyl oxygen belonging to the ester group. In contrast,

dx.doi.org/10.1021/jp304212y | J. Phys. Chem. A 2012, 116, 12389–12398

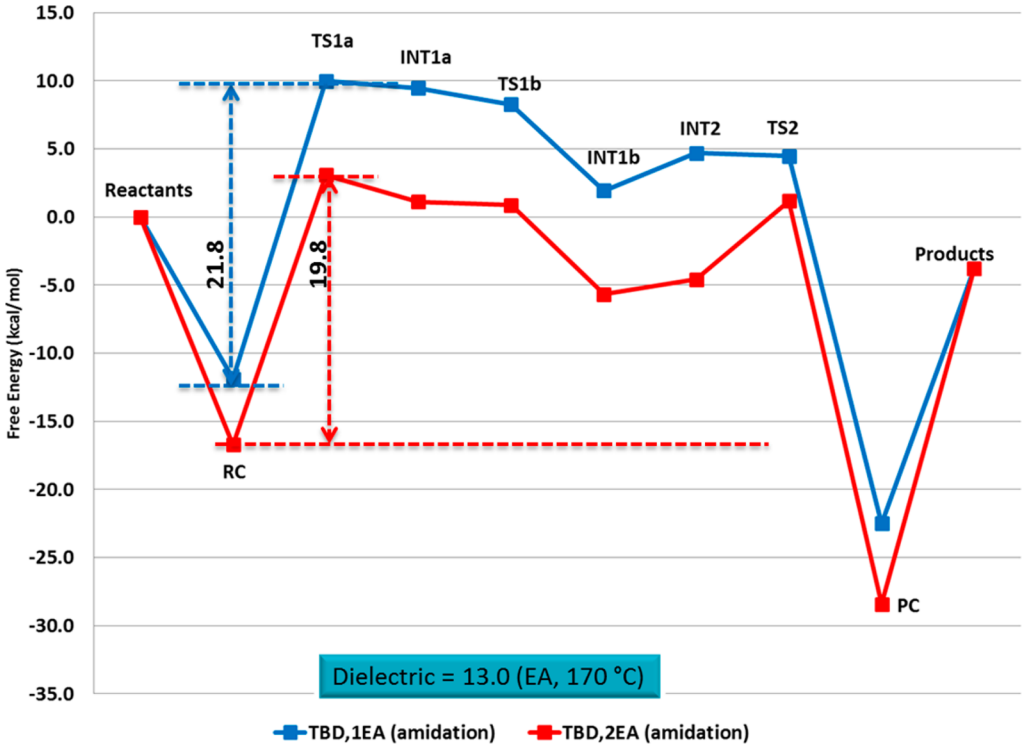

Figure 8. Reaction profile for the amidation of MB with EA catalyzed by TBD and TBD + EA.

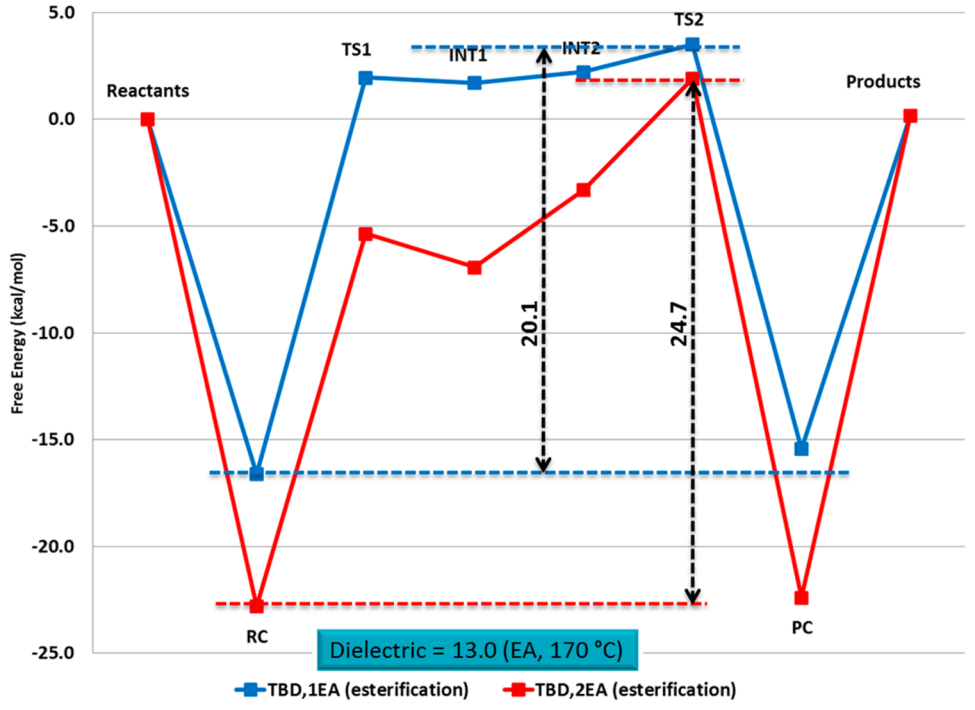

Figure 9. Reaction profile for the trans-esterification of MB with EA catalyzed by TBD and TBD + EA.

in transition states involving the TBD + EG or DBU + EG cocatalysts, the EG cocatalyst binds to the carbonyl oxygen, while TBD (or DBU) are bound to the attacking hydroxyl group. The interactions involving the pendant hydroxyl group belonging to the diol are also noteworthy. When TBD acts as a lone catalyst, the pendant hydroxyl group does not interact with hydrogen-bond acceptors on the ester. However, when a cocatalyst is used with TBD and DBU, the orientation of the catalytic base allows the pendant hydroxyl group on the diol to stabilize developing negative charge on the carbonyl oxygen during nucleophilic attack. Two factors may be responsible for the similarity of the barriers observed for all three mechanisms. First, while addition of a cocatalyst provides additional stabilization of the transition state, this is counterbalanced by the destabilization caused by entropic or steric factors. Second, as we pointed out previously for reactions involving EDA, while

dx.doi.org/10.1021/jp304212y | J. Phys. Chem. A 2012, 116, 12389−12398

transition structures are stabilized by the addition of a cocatalyst, the reactant complex is stabilized to almost the same extent. As a result, the barriers for all three mechanisms are very similar.

Transition structures for nucleophilic attack by EG on the ester are early according to the Hammond postulate. For the reaction catalyzed by TBD + EG, the O−H bond is completely broken, and the proton is already completely transferred to the organocatalyst, while the bond distance for the forming C−O bond is ≥2 Å. The vibrational mode for this TS shows that the proton, which had already been transferred, does not move while the C−O bond is being formed. The TS motion for the reaction catalyzed by DBU + EG shows that proton transfer from the alcohol occurs at the same time as formation of the C−O bond. These results are in stark contrast with results involving EDA in which C−N bond formation precedes proton transfer in two distinct transition structures.

Our calculations predict that the catalytic activities of TBD and DBU in the trans-esterification of MB with EG are very similar, within computational error. This prediction is not quite in agreement with experiments showing that DBU is more active than TBD in the glycolysis of PET (Figure 1a).[53]

It is possible that more reliable computational results could be obtained by using more accurate methods to reproduce the experimentally observed catalytic activities. One potential source of improvement is the solvation procedure used to model these reactions. EG, EA, and EDA are highly hydrogen-bonding, polar solvents, that may not be accurately modeled by the continuum dielectric model even after inclusion of an explicit solvent molecule in the model since these models cannot accurately describe the strong intermolecular hydrogen-bond network that must exist in these high boiling point solvents. More accurate computational models for these reactions would possibly involve the calculation of free energies using molecular dynamics (MD) simulations with methods such as ab initio Carr−Parrinello MD[54] or the use of a QM/MM approach in which the solute and solvent shell are described at the DFT-D level of theory, while the classical solvent is described using an all-atom force field that properly accounts for long-range Lennard-Jones and Coulomb interactions (including Ewald interactions between classical point charges and the QM wave function up to the quadrupole configuration).[55] However, the use of sophisticated models such as the aforementioned is impractical given present-day software and hardware capabilities.

Amidation and Trans-Esterification of MB with EA. Only reactions involving TBD as the sole catalyst or involving the cocatalyst combination of TBD + EA have been examined in reactions of MB with EA. Since amide and ester formation are competing processes in the reactions of EA with MB, we have computed both the N-selective and O-selective pathways to determine why amidation is experimentally favored in these reactions. These pathways are shown in Figures 8 and 9, respectively.

Similar to reactions involving EDA, nucleophilic attack during amidation by EA occurs in two stages, first C−N bond formation in TS1a followed by proton transfer in TS1b. As shown in Figure 8, nucleophilic attack in TS1a is rate-determining whether TBD acts as the lone catalyst in the amidation of MB by EA (barrier = 22 kcal/mol) or when EA is used as a cocatalyst with TBD (barrier = 20 kcal/mol).

Transition states for methanol loss, TS2, are rate-determining in mechanisms involving the TBD-catalyzed trans-esterification of MB with EA. The barrier for TBD-catalyzed methanol loss is 20 kcal/mol (Figure 9). This barrier *increases* to 25 kcal/mol with the use of an additional molecule of EA as a cocatalyst, likely caused by the fact that the reactant complex is more stabilized than the transition state by hydrogen-bonding interactions introduced with the addition of the molecule of EA.

Barriers for the rate-determining steps in the trans-esterification and amidation pathways are approximately 20 kcal/mol. This suggests that the yields of amide and ester would be approximately the same, contrary to experiments demonstrating that no esterification product is formed and that the amide is exclusively favored during the depolymerization of PET with EA (see Figure 1c).

Significantly, however, the trans-esterification of MB with EA is slightly endergonic, while amidation is exergonic; the reaction free energies of these processes are +0.2 and −3.8 kcal/mol, respectively. Moreover, the rate-determining barriers for the reverse trans-esterification pathway (involving the TBD-catalyzed reaction of the ester product, 2-aminoethyl benzoate, with methanol, i.e., the transformation of PC to INT2 via TS2) are 19−24 kcal/mol, while the barriers for the analogous process involving the amide are 27−30 kcal/mol. Overall, these results suggest that the trans-esterification and amidation pathways for the reaction of MB with EA are equally likely in kinetic terms, but trans-esterification is reversible, while the amide forms a more stable amide product, which is less likely to revert to starting materials. Therefore, computational results predict that the reaction of MB with EA results in the exclusive formation of the amide, which is in agreement with experimental results.

■ CONCLUSIONS

We have studied the TBD- and DBU-catalyzed trans-esterification and amidation of MB with EG, EDA, and EA with density functional theory. These are model systems for the depolymerization of PET with esters and amides. Our investigations suggest that the introduction of a cocatalyst in these reactions by the use of excess reagent leads to a slight increase in the rate of reaction or actually decreases the rate in those cases in which the transition state becomes more sterically hindered. It appears that the requirement of excess solvent in experiment is primarily for thermodynamic purposes according to Le Chatelier's principle.

DBU is typically less active than TBD in amidation reactions, which is in agreement with experimental observations. However, our computational predictions suggest that TBD and DBU possess similar catalytic activity in the esterification of methyl benzoate, while experiments suggest that DBU is a more active catalyst in the esterification of PET with EG.

We also demonstrate that esterification by EG is more favorable than amidation by EDA because the catalysts activate alcohols more than amines during nucleophilic attack. Alcohols are completely deprotonated by the catalytic base TBD forming alkoxides during nucleophilic attack leading to lower barriers than those observed for amines. However, nucleophilic attack by amines is accomplished in two stages; the C−N bond is first formed before the amine becomes deprotonated in a subsequent transition state. Calculations predict that the amide product is formed in the TBD-catalyzed reaction of EA with MB in agreement with experiment because, although the barriers are very similar, trans-esterification is reversible, while the thermodynamic product is formed by amidation.

■ ASSOCIATED CONTENT

Supporting Information

Experimental details, characterization data, B3LYP-optimized Cartesian coordinates, and electronic energies (hartrees) for all stationary points. This material is available free of charge via the Internet at http://pubs.acs.org.

■ AUTHOR INFORMATION

Corresponding Author

*E-mail: hanshorn@us.ibm.com.

Notes

The authors declare no competing financial interest.

■ REFERENCES

(1) United States Environmental Protection Agency. Municipal Solid Waste Generation, Recycling, and Disposal in the United States: Facts and Figures for 2009, December 2010. http://www.epa.gov/osw/nonhaz/municipal/pubs/msw2009-fs.pdf (accessed 6/17/2011).

(2) National Association for PET Container Resources. 2009 Report on Post-Consumer PET Container Recycling Activity. National Association for PET Container Resources, October 20, 2010. http://www.napcor.com/pdf/2009_Report.pdf (accessed 6/17/2011).

(3) American Chemistry Council. 2009 United States National Post-Consumer Plastics Bottle Recycling Report. 2010. http://plastics.americanchemistry.com/09-Post-Consumer-Plastics-Bottle-Recycling-Rpt (accessed 6/17/2011).

(4) Scheirs, J. In *Polymer Recycling: Science, Technology and Applications*; Scheirs, J., Ed.; Wiley: New York, 1998; Chapter 4, pp 119−182.

(5) Mancini, S. D.; Zanin, M. *Mater. Res.* **1999**, *2*, 33.

(6) Cornell, D. D. In *Modern Polyesters: Chemistry and Technology of Polyesters and Copolyesters*, Scheirs, J., Long, T. E., Eds.; Wiley: New York, 2003; Chapter 16, pp 565−587.

(7) Paszun, D.; Spychaj, T. *Ind. Eng. Chem. Res.* **1997**, *36*, 1373−1383.

(8) Klein, P. In *Recycling and Recovery of Plastics*; Brandrup, J., Bittner, M., Menges, G., Michaeli, W., Eds.; Hanser Gardner Publications: Cincinnati, OH, 1996; Chapter 5, pp 494−502.

(9) Farahat, M. S.; Nikles, D. E. *Macromol. Mater. Eng.* **2001**, *286*, 695−704.

(10) Vaidya, U. R.; Nadkarni, V. M. *Ind. Eng. Chem. Res.* **1987**, *26*, 194−198.

(11) Shukla, S. R.; Harad, A. M.; Jawale, L. S. *Waste Manage.* **2008**, *28*, 51−56.

(12) Halacheva, N.; Novakov, P. *Polymer* **1995**, *36*, 867−874.

(13) Pardal, F.; Tersac, G. *Polym. Degrad. Stab.* **2006**, *91*, 2567−2578.

(14) Chen, C. H.; Chen, C. Y.; Lo, U. W.; Mao, C. F.; Liao, W. T. *J. Appl. Polym. Sci.* **2001**, *80*, 943−948.

(15) Baliga, S.; Wong, W. T. *J. Polym. Sci., Part A: Polym. Chem.* **1989**, *27*, 2071−2082.

(16) Kamber, N. E.; Jeong, W.; Waymouth, R. M.; Pratt, R. C.; Lohmeijer, B. G. G.; Hedrick, J. L. *Chem. Rev.* **2007**, *107*, 5813−5840.

(17) Kiesewetter, M. K.; Shin, E. J.; Hedrick, J. L.; Waymouth, R. M. *Macromolecules* **2010**, *43*, 2093−2107.

(18) Kamber, N. E.; Tsuji, Y.; Keets, K.; Waymouth, R. M.; Pratt, R. C.; Nyce, G. W.; Hedrick, J. L. *J. Chem. Educ.* **2010**, *87*, 519−521.

(19) Pratt, R. C.; Lohmeijer, B. G.; Long, D. A.; Waymouth, R. M.; Hedrick, J. L. *J. Am. Chem. Soc.* **2006**, *128*, 4556−4557.

(20) Lohmeijer, B. G. G.; Pratt, R. C.; Leibfarth, F.; Logan, J. W.; Long, D. A.; Dove, A. P.; Nederberg, F.; Choi, J.; Wade, C.; Waymouth, R. M.; Hedrick, J. L. *Macromolecules* **2006**, *39*, 8574−8583.

(21) Nederberg, F.; Lohmeijer, B. G. G.; Leibfarth, F.; Pratt, R. C.; Choi, J.; Dove, A. P.; Waymouth, R. M.; Hedrick, J. L. *Biomacromolecules* **2007**, *8*, 153.

(22) Pratt, R.; Nederberg, F.; Waymouth, R. M.; Hedrick, J. L. *Chem. Commun.* **2008**, 114−116.

(23) Kiesewetter, M. K.; Scholten, M. D.; Kirn, N.; Weber, R. L.; Hedrick, J. L.; Waymouth, R. M. *J. Org. Chem.* **2009**, *74*, 9490−9496.

(24) Coady, D. J.; Fukushima, K.; Horn, H. W.; Rice, J. E.; Hedrick, J. L. *Chem. Commun.* **2011**, *47*, 3105−3107.

(25) Fukushima, K.; Coulembier, O.; Lecuyer, J. M.; Almegren, H. A.; Alabdulrahman, A. M.; Alsewailem, F. D.; McNeil, M. A.; DuBois, P.; Waymouth, R. M.; Horn, H. W.; Rice, J. E.; Hedrick, J. L. *J. Polym. Sci., Part A: Polym. Chem.* **2011**, *49*, 1273−1281.

(26) Fukushima, K.; Lecuyer, J. M.; Wei, D. S.; Horn, H. W.; Jones, G. O.; Almegren, H. A.; Mohammad, A. M.; Alsewailem, F. D.; McNeil, M. A.; Rice, J. E.; Hedrick, J. L. *Polymer Chemistry*, in press.

(27) Garnish, E. W. In *Structural Adhesives: Developments in Resins and Primers*; Kinloch, A. J., Ed.; Elsevier Applied Science Publishers: New York, 1986; Chapter 3, pp 57−76.

(28) Anderson, C. C. *Ind. Eng. Chem.* **1968**, *60*, 80−87.

(29) Note that the relative reactivity referred to here is not dependent on measurement of absolute rates, but on the time observed for reaction completion (i.e., when PET flakes disappear) or on the yields of product formed by reactions catalyzed by the respective catalysts for a set duration of reaction. To be specific, depolymerization products precipitate and crystallize during amidation with EDA. As a result, the exact completion point of PET depolymerization during amidation with EDA was difficult to determine. See Supporting Information for details.

(30) Chuma, A.; Horn, H. W.; Swope, W. C.; Pratt, R. C.; Zhang, L.; Lohmeijer, B. G. G.; Wade, C. G.; Waymouth, R. M.; Hedrick, J. L.; Rice, J. E. *J. Am. Chem. Soc.* **2008**, *130*, 6749−6754.

(31) Dove, A. P.; Pratt, R. C.; Lohmeijer, B. G. G.; Waymouth, R. M.; Hedrick, J. L. *J. Am. Chem. Soc.* **2005**, *127*, 13798−13799.

(32) Simón, L.; Goodman, J. M. *J. Org. Chem.* **2007**, *72*, 9656−9662.

(33) Buis, N.; French, S. A.; Ruggiero, G. D.; Stengel, B.; Tulloch, A. A. D.; Williams, I. H. *J. Chem. Theory Comput.* **2007**, *3*, 146−155.

(34) Jin, L.; Wu, Y.; Kim, C.-K.; Xue, Y. *J. Mol. Struct.* **2010**, *942*, 137−144.

(35) Schmidt, M. W.; Baldridge, K. K.; Boatz, J. A.; Elbert, S. T.; Gordon, M. S.; Jensen, J. H.; Koseki, S.; Matsunaga, N.; Nguyen, K. A.; Su, S. J.; Windus, T. L.; Dupuis, M.; Montgomery, J. A. *J. Comput. Chem.* **1993**, *14*, 1347−1363.

(36) The General Atomic and Molecular Electronic Structure System (GAMESS), v2009R1 and v2010R3; see http://www.msg.ameslab.gov/GAMESS/GAMESS.html.

(37) Becke, A. D. *J. Chem. Phys.* **1993**, *98*, 5648−5652.

(38) Lee, C.; Yang, W.; Parr, R. G. *Phys. Rev. B* **1988**, *37*, 785−789.

(39) Vosko, S. H.; Wilk, L.; Nusair, M. *Can. J. Phys.* **1980**, *58*, 1200−1211.

(40) Stephens, P. J.; Devlin, F. J.; Chabalowski, C. F.; Frisch, M. J. *J. Phys. Chem.* **1994**, *98*, 11623−11627.

(41) Hehre, W. J.; Ditchfield, R.; Pople, J. A. *J. Chem. Phys.* **1972**, *56*, 2257−2261.

(42) Hariharan, P. C.; Pople, J. A. *Theor. Chim. Acta* **1973**, *28*, 213−222.

(43) Clark, T.; Chandrasekhar, J.; Spitznagel, G. W.; Schleyer, P. v. R. *J. Comput. Chem.* **1983**, *4*, 294−301.

(44) Woon, D. E.; Dunning, T. H., Jr. *J. Chem. Phys.* **1995**, *103*, 4572−4585.

(45) Kendall, R. A.; Dunning, T. H., Jr.; Harrison, R. J. *J. Chem. Phys.* **1992**, *96*, 6796−6806.

(46) Schafer, A.; Horn, H.; Ahlrichs, R. *J. Chem. Phys.* **1992**, *97*, 2571−2577. Diffuse s,p functions were added via extrapolation.

(47) Barone, V.; Cossi, M. *J. Phys. Chem. A* **1998**, *102*, 1995−2001.

(48) Cossi, M.; Rega, N.; Scalmani, G.; Barone, V. *J. Comput. Chem.* **2003**, *24*, 669−681.

(49) Mennucci, B. Personal communication; e-mail: bene@dcci.unipi.it.

(50) Permittivity; Dielectric Constants of Liquids. In *CRC Handbook of Chemistry and Physics*, 84th ed.; CRC Press: Boca Raton, FL, 2003; Vol. *1*, pp 6-155−6-177.

(51) Ribeiro, R. F.; Marenich, A. V.; Cramer, C. J.; Truhlar, D. G. *J. Phys. Chem. B* **2011**, *115*, 14556−14562.

(52) In our previous investigation (ref 25), we used dimethylterephthalate as a model for PET and methanol as a model for ethylene glycol. Those investigations suggested that the additional ester group present in the terephthalate model was not required for the investigation of the mechanisms of these reactions. However, we deemed it necessary that more complete computational models for amine or alcohol reagents needed to be included because of large differences in nucleophile basicity and nucleophilicity.
(53) We obtained similar results (for the barrier heights) by using B3LYP-D3, a method that accounts for dispersion and for predictions of catalytic activity in the TBD and DBU-catalyzed reactions of EG with MB. For details about B3LYP-D3, see Grimme, S.; Anthony, J.; Ehrlich, S.; Krieg, H. *J. Chem. Phys.* **2010**, *132*, 154104−154119.
(54) Car, R.; Parrinello, M. *Phys. Rev. Lett.* **1985**, *55*, 2471−2474.
(55) Hammes-Schiffer, S. Ph.D. Dissertation, Stanford University, 1993.